

A new scalar mediated WIMPs with pairs of on-shell mediators in annihilations

Lian-Bao Jia^{*}

School of Science, Southwest University of Science and Technology, Mianyang 621010, P. R. China

Abstract

In this article, we focus on a new scalar ϕ mediated scalar/vectorial WIMPs (weakly interacting massive particles). To explain the Galactic center 1 - 3 GeV gamma-ray excess, here we consider the case that a WIMP pair predominantly annihilates into an on-shell $\phi\phi$ pair which mainly decays to $\tau\bar{\tau}$, with masses of WIMPs in a range about 14 - 22 GeV. For the mass of ϕ slightly below the WIMP mass, the annihilations of WIMPs are phase space suppressed today, and the required thermally averaged annihilation cross section of WIMPs can be derived to meet the GeV gamma-ray excess. A small scalar mediator-Higgs field mixing is introduced, which is available in interpreting the GeV gamma-ray excess. With the constraints of the dark matter relic density, the indirect detection result, the collider experiment, the thermal equilibrium of the early universe and the dark matter direct detection experiment are considered, we find there are parameter spaces left. The WIMPs may be detectable at the upgraded dark matter direct detection experiment in the next few years, and the signature of ϕ may be observable via ϕ strahlung at future high-luminosity e^+e^- collider.

^{*}Electronic address: jialb@mail.nankai.edu.cn

I. INTRODUCTION

The weakly interacting massive particle (WIMP) type dark matter (DM) attracts much attention in DM direct detections, and the cold DM relic density can be derived from thermally freeze-out WIMPs. Today, the compatible confident events are still absent in DM direct detection experiments, and the recent search results of CRESST-II [1], CDMSlite [2], LUX [3] and XENON1T [4] set stringent constraints on the WIMP-nucleus spin-independent (SI) scattering. For WIMPs, novel scenarios are needed to escape the present direct detection constraints.

The cosmic ray observations, such as γ -rays, neutrinos, positrons, and antiprotons from DM dense regions, may indirectly reveal properties of WIMPs. The recent 1-3 GeV gamma-ray excess from the Galactic center may be due to WIMP annihilations, for WIMPs in a mass range about 35-50 GeV annihilating into $b\bar{b}$ with corresponding annihilation cross section $\sim (1 - 3) \times 10^{-26} \text{ cm}^3/\text{s}$ [5-7], or WIMPs in a mass range about 7 -11 GeV annihilating into $\tau\bar{\tau}$ with the annihilation cross section $\sim 0.5 \times 10^{-26} \text{ cm}^3/\text{s}$ (20% to $b\bar{b}$ also allowed) [5-8]. In this work, we focus on the latter case, that is, the main WIMP annihilation products in the standard model (SM) sector are $\tau\bar{\tau}$ pairs (see Refs. [9-12] for more discussions). Moreover, with a small number of visible matter in dwarf satellite galaxies, gamma rays from the DM-dominant dwarf galaxies provide significant information about WIMPs. The $\tau\bar{\tau}$ mode galactic center GeV gamma-ray excess is compatible with the results from the Fermi-LAT new dwarf galaxy observations [13].

New physics beyond SM is needed to yield the main product $\tau\bar{\tau}$ in SM sector in WIMP annihilations. The leptophilic WIMPs were discussed in the literature [14-23]. Here we consider that a new scalar can mediate the interactions between SM charged leptons and scalar/vectorial WIMPs (the annihilation of fermionic WIMPs is p-wave suppressed today), and the new couplings of the mediator to leptons are proportional to the lepton masses. If the scalar mediator is lighter than the WIMP mass, the way of a WIMP pair annihilating into an on-shell mediator pair is allowed (see e.g. Refs. [24, 25] for more). In this case, the scalar mediator's couplings to SM particles can be almost arbitrarily small.¹ To fit the GeV gamma-ray excess and meanwhile evade present constraints from DM direct detections and collider experiments, we focus on the case that the mediator is lighter than the WIMP mass and the mediator-tau lepton coupling is much smaller than the mediator-WIMP coupling. Thus, the dominant annihilation mechanism of WIMPs is that a WIMP pair annihilates into an on-shell mediator pair which mainly decays to the heaviest leptons $\tau\bar{\tau}$. The case of $\tau\bar{\tau}$ mode dominant is naturally compatible with the antiproton spectrum observations from PAMELA [26], and is tolerant by the smooth positron spectrum of AMS-02 [27-29].

A small scalar mediator-Higgs field mixing is discussed, and the mixing is small enough to keep $\tau\bar{\tau}$ dominant in the scalar mediator decay. With a small mixing introduced, one prospect is that the WIMP-target nucleus scattering may be detectable at the upgraded DM direct detection experiment in the next few years, and another prospect is that the scalar mediator may be observable in the future high-luminosity e^+e^- experiment. In fact, the small mediator-Higgs

¹ There is a lower bound about the couplings, which is from the thermal equilibrium in the early universe.

mixing can play an important role in the thermal equilibrium of the early universe. The reaction rates of SM particles \rightarrow WIMPs should be larger than the expansion rate of the universe, and this sets a lower bound about the couplings of the scalar mediator to SM particles. These will be explored in this paper.

This work is organized as follows. After this introduction, the form of the interactions in new sector and the annihilation cross section of scalar/vectoral WIMPs are given in section II. Next we give a detailed analysis about scalar WIMPs in section III, including the constraints and the test at future experiment. In section IV, we give a brief discussion about the test of vectoral WIMPs. The conclusions and some discussions are given in the last section.

II. INTERACTIONS BETWEEN WIMPS AND SM

In this article, we focus on scalar/vectoral WIMPs, with a new scalar field mediating the interactions between WIMPs and SM particles.

A. The new sector interactions

Here we formulate the corresponding interactions. Following the forms in Refs [30–33], the effective interactions of a real scalar field Φ to scalar/vectoral WIMPs, charged lepton l (e, μ, τ) and Higgs field are taken as

$$\mathcal{L}_S^i = -\frac{\lambda}{2}\Phi^2 S^* S - \mu\Phi S^* S - \lambda_l\Phi\bar{l}l - \lambda_h\Phi^2(H^\dagger H - \frac{v^2}{2}) - \mu_h\Phi(H^\dagger H - \frac{v^2}{2}), \quad (1)$$

$$\mathcal{L}_V^i = \frac{\lambda}{2}\Phi^2 V_\mu^* V^\mu + \mu\Phi V_\mu^* V^\mu - \lambda_l\Phi\bar{l}l - \lambda_h\Phi^2(H^\dagger H - \frac{v^2}{2}) - \mu_h\Phi(H^\dagger H - \frac{v^2}{2}), \quad (2)$$

where S is a scalar WIMP field, V^μ is a vectoral WIMP field, and a Z_2 symmetry is introduced to let WIMPs stable. The Yukawa type coupling parameter λ_l is proportional to the charged lepton mass. H is the Higgs field, v is the vacuum expectation value with $v \approx 246$ GeV, and Φ is chosen for no vacuum expectation value obtained [30, 31]. The parameter μ can be rewritten as $\mu = km_S$, $\mu = km_V$, with k a dimensionless parameter and m_S, m_V the scalar, vectoral WIMP mass respectively. The scalar component h' of Higgs field and the scalar field Φ can mix after the electroweak symmetry breaking, giving the mass eigenstates h, ϕ in the form

$$\begin{pmatrix} h \\ \phi \end{pmatrix} = \begin{bmatrix} \cos\theta & \sin\theta \\ -\sin\theta & \cos\theta \end{bmatrix} \begin{pmatrix} h' \\ \Phi \end{pmatrix}. \quad (3)$$

Here θ is the mixing angle, and one has

$$\tan 2\theta = \frac{2v\mu_h}{m_\Phi^2 + \lambda_h v^2 - m_H^2}. \quad (4)$$

To be compatible with experimental constraints, θ is small, i.e. $\cos\theta \sim 1$, $\sin\theta \sim \theta \ll 1$. The θ value should be small enough to keep $\tau\bar{\tau}$ dominant in WIMP pair annihilating into SM products.

B. Annihilations of WIMPs

The case the scalar mediator is lighter than the WIMP mass $m_\phi < m_S, m_V$, is of our concern in this paper. When the coupling $\lambda, k^2 \gg k\lambda_\tau$, a WIMP pair predominantly annihilates into an on-shell $\phi\phi$ pair. The ϕ particle mainly decays to $\tau\bar{\tau}$, and the gamma rays from $\tau\bar{\tau}$ mode can reveal some properties of WIMPs. The differential gamma-ray flux from DM annihilation is

$$E_\gamma^2 \frac{d\Phi_\gamma}{dE_\gamma} = \frac{\langle\sigma_{ann}v_r\rangle_0 J}{8\pi m_{DM}^2} \sum_i BR_i E_\gamma^2 \frac{dN_\gamma^i}{dE_\gamma}, \quad (5)$$

where $\langle\sigma_{ann}v_r\rangle_0$ is the thermally averaged DM annihilation cross section today, and J is the annihilation J -factor. In the scenario of WIMP pair $\rightarrow \phi\phi$, to fit the galactic center gamma-ray excess via $\tau\bar{\tau}$ mode as mentioned by the introduction, the WIMP mass is twice, i.e. about 14-22 GeV, and the thermally averaged annihilation cross section today is about $1 \times 10^{-26} \text{ cm}^3/\text{s}$ (i.e. nearly 1/2 of that at the thermally freeze-out temperature), with the ϕ mass m_ϕ close to the WIMP mass m_S, m_V .

1. Scalar WIMPs

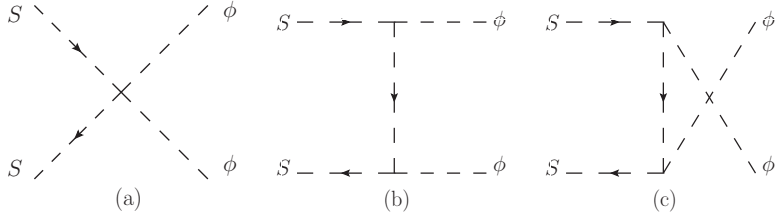


FIG. 1: The process of $SS^* \rightarrow \phi\phi$.

Let us consider the scalar WIMPs first. The process $SS^* \rightarrow \phi\phi$ is dominant in the WIMP annihilation, as shown in Fig. 1. The WIMP annihilation cross section in one particle rest frame is

$$\sigma_{ann}v_r \simeq \frac{1}{2} \frac{\beta_f}{32\pi(s - 2m_S^2)} \left(\lambda + 2k^2 \frac{m_S^2}{m_\phi^2 - 2m_S^2} \right)^2. \quad (6)$$

Here the factor $\frac{1}{2}$ arises from the required SS^* type in annihilations, v_r is the relative velocity of two WIMP particles, and s is the total invariant mass squared. β_f is a kinematic factor, with

$$\beta_f = \sqrt{1 - \frac{4m_\phi^2}{s}}. \quad (7)$$

Due to the β_f factor, when the mediator mass m_ϕ is slightly below the WIMP mass m_S , i.e. being close to the threshold of $SS^* \rightarrow \phi\phi$, the thermally averaged annihilation cross section $\langle\sigma_{ann}v_r\rangle_0$ today (in the $T = 0$ limit) is more suppressed in phase space compared with the cross

section $\langle\sigma_{ann}v_r\rangle_f$ at the freeze-out temperature T_f . For this thermally freeze-out case, the key factor β_f is failed to be expanded in Taylor series of v_r^2 .

The present DM relic density Ω_D and the parameter x_f (with $x_f = m_S/T_f$) can be approximately written as [34, 35]

$$\Omega_D h^2 \simeq \frac{1.07 \times 10^9 \text{ GeV}^{-1}}{J_{ann} \sqrt{g_*} m_{\text{Pl}}}, \quad (8)$$

$$x_f \simeq \ln 0.038 c(c+2) \frac{g m_{\text{Pl}} m_S \langle\sigma_{ann}v_r\rangle_f}{\sqrt{g_* x_f}}, \quad (9)$$

with

$$J_{ann} = \int_{x_f}^{\infty} \frac{\langle\sigma_{ann}v_r\rangle}{x^2} dx. \quad (10)$$

Here h is the Hubble constant (in units of 100 km/(s·Mpc)), and g_* is the number of the relativistic degrees of freedom with masses less than the temperature T_f . m_{Pl} is the Planck mass with the value 1.22×10^{19} GeV, and g is the degrees of freedom of DM. The parameter c is of order one, and $c = 1/2$ is taken here. The thermally averaged annihilation cross section is [36, 37]

$$\begin{aligned} \langle\sigma_{ann}v_r\rangle &= \frac{2x}{K_2^2(x)} \int_0^{\infty} d\varepsilon \sqrt{\varepsilon} (1+2\varepsilon) \\ &\quad \times K_1(2x\sqrt{1+\varepsilon}) \sigma_{ann} v_r, \end{aligned} \quad (11)$$

with $\varepsilon = (s - 4m_S^2)/4m_S^2$. K_i is the i -th order modified Bessel function.

2. Vectoral WIMPs

Now let us turn to the vectoral WIMPs. The process $VV^* \rightarrow \phi\phi$ is dominant in the vectoral WIMP annihilation. When m_ϕ is slightly below m_V , the annihilation cross section is

$$\sigma_{ann} v_r \simeq \frac{1}{2} \frac{\beta_f}{96\pi(s-2m_V^2)} (\lambda + 2k^2 \frac{m_V^2}{m_\phi^2 - 2m_V^2})^2. \quad (12)$$

For vectoral WIMPs, the thermally averaged annihilation cross section, the relic density are similar to the scalar case, with the corresponding parameter inputs in calculations.

III. ANALYSIS OF SCALAR WIMPS

Here we give a detailed analysis about the scalar WIMPs, and the case of vectoral WIMPs is similar.

A. The constraints of WIMP annihilations

The process of WIMP pair $\rightarrow \phi\phi$ is dominant in WIMP annihilations. For the $\tau\bar{\tau}$ mode in WIMP annihilations, the present thermally averaged cross section set by the Galactic center gamma-ray excess is $\langle\sigma_{ann}v_r\rangle_0 \sim 1 \times 10^{-26} \text{ cm}^3/\text{s}$, with the mass of WIMPs in the range 14-22 GeV. The cold DM relic density today is $\Omega_c h^2 = 0.1197 \pm 0.0022$ [38]. These constraints are taken to restrict the parameter spaces.

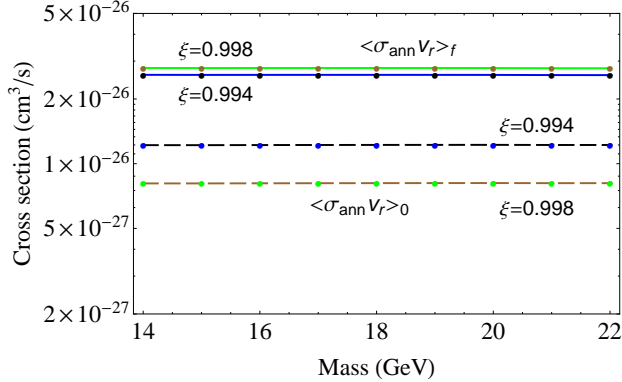


FIG. 2: The thermally averaged annihilation cross section of WIMPs with masses in the range 14 - 22 GeV. The solid-dotted curves are the results of $\langle\sigma_{ann}v_r\rangle_f$, with the lower one, the upper one corresponding to the case of $\xi = 0.994$, $\xi = 0.998$, respectively. The dashed-dotted curves are the results of $\langle\sigma_{ann}v_r\rangle_0$, with the upper one, the lower one for the case of $\xi = 0.994$, $\xi = 0.998$, respectively.

Define $m_\phi/m_S = \xi$, with $\xi < 1$ and ξ close to 1. The factor β_f plays a key role in fixing the ratio $\langle\sigma_{ann}v_r\rangle_0/\langle\sigma_{ann}v_r\rangle_f$, and the value of ξ can be set by $\Omega_c h^2$ and $\langle\sigma_{ann}v_r\rangle_0$. The numerical results of the thermally averaged annihilation cross sections are shown in Fig. 2, for WIMP masses in the range 14-22 GeV. When ξ changes in the range $0.994 \lesssim \xi \lesssim 0.998$, $\langle\sigma_{ann}v_r\rangle_0$ approximately varies from $1.2 \times 10^{-26} \text{ cm}^3/\text{s}$ to $0.8 \times 10^{-26} \text{ cm}^3/\text{s}$. The derived annihilation cross section range of $\langle\sigma_{ann}v_r\rangle_0$ together with the WIMP mass range of concern can give an interpretation about the Galactic center GeV gamma-ray excess.

Since the value of ξ is obtained by the constraints, the coupling between WIMPs and the mediator ϕ is also determined. Taking $\xi \sim 0.994$, we have

$$|\lambda - 2k^2| \sim 2.0 \times 10^{-3} m_S(\text{GeV}), \quad (13)$$

with m_S in units of GeV. The coupling μ in the WIMP- ϕ trilinear term plays an important role in the WIMP-target nucleus scattering in DM direct detections. In the case of the trilinear term dominant in WIMP annihilations, we have

$$k = \frac{\mu}{m_S} \sim 3.16 \times 10^{-2} \sqrt{m_S(\text{GeV})}. \quad (14)$$

If the contribution from λ term is significant in WIMP annihilations, the relation

$$\lambda \sim 2k^2 \pm 2.0 \times 10^{-3} m_S \quad (15)$$

needs to be taken care of. In the case of a large λ value together with a comparable large k , the s-channel WIMP annihilation is enhanced. As we focus on the s-channel suppressed case in this paper, e.g. the value $\lambda + 2k^2$ being order of $2.0 \times 10^{-3}m_S$, and here a range of k

$$k^2 \lesssim 1.4 \times 10^{-3}m_S(\text{GeV}), \quad (16)$$

is considered in calculations.

B. The constraints of ϕ

Now we give a brief discussion about the coupling of ϕ to SM particles, that is, the λ_τ 's value and the mixing angle θ . Some parameters are inputted as follows, $m_\tau = 1.77682$ GeV, $m_\mu = 0.105658$ GeV, $m_t = 173.21$ GeV, $m_b = 4.18$ GeV, with the results from PDG [39].

1. The λ_τ value

As discussed above, the case of s-channel suppressed in WIMP annihilations is of our concern, i.e. $\lambda, k^2 \gg k\lambda_\tau$. Here the k value in μ term dominant case is taken to restrict the λ_τ 's value, that is

$$\lambda_\tau \ll 3.16 \times 10^{-2} \sqrt{m_S(\text{GeV})}. \quad (17)$$

The decay width of ϕ is

$$\Gamma_\phi \simeq \frac{m_\phi}{8\pi} [\lambda_\tau^2 (1 - \frac{4m_\tau^2}{m_\phi^2})^{3/2} + 3\frac{m_b^2}{v^2} \sin^2 \theta (1 - \frac{4m_b^2}{m_\phi^2})^{3/2}], \quad (18)$$

with λ_τ term dominant. Taking the limit of λ_τ in Eq. (17), we have $\Gamma_\phi \ll (m_S - m_\phi)$. Thus, the ξ 's range of concern is feasible.

The ϕ particle contributes to the muon $g - 2$, and the one-loop result is [40]

$$a_\mu^\phi \simeq \frac{\lambda_\mu^2}{8\pi^2} \frac{m_\mu^2}{m_\phi^2} \left(\ln \frac{m_\phi^2}{m_\mu^2} - \frac{7}{6} \right). \quad (19)$$

The difference between experiment and theory is [39]

$$\Delta a_\mu = a_\mu^{\text{exp}} - a_\mu^{\text{SM}} = 288(63)(49) \times 10^{-11}. \quad (20)$$

Taking the replacement $\lambda_\mu = \lambda_\tau m_\mu / m_\tau$ and $m_\phi \sim m_S$ in Eq. (19), we can find that the upper limit of λ_τ in Eq. (17) is tolerant by the muon $g - 2$ result.

2. The mixing angle θ

For the WIMP mass range of concern, according to Eq. (18), if the $b\bar{b}$ channel is not larger than 20%, the θ value should satisfy the relation $\sin \theta \lesssim 20\lambda_\tau$ (when λ_τ is compatible with 0.01, this constraint is relaxed). The Higgs hunt results at LEP [41] set an upper limit on θ ,

$$\sin^2 \theta \lesssim 0.1 \ (\phi \rightarrow \tau\bar{\tau}), \quad \sin^2 \theta \mathcal{B}_{\phi \rightarrow b\bar{b}} \lesssim 2 \times 10^{-2}. \quad (21)$$

We can see that the constraints from LEP are mild. The ATLAS [42] and CMS [43] search constraints about light Higgs-like particles can be approximately written as [44, 45]

$$\sin^2 \theta \mathcal{B}_{\phi \rightarrow \mu^+ \mu^-} \lesssim \mathcal{B}_{h \rightarrow \mu^+ \mu^-}^{SM}. \quad (22)$$

With these constraints, we obtain an upper limit of θ

$$\sin^2 \theta \lesssim 6 \times 10^{-2}, \quad \text{and} \quad \sin \theta \lesssim 20\lambda_\tau. \quad (23)$$

The constraints of the DM direct detection and Higgs boson decay will be discussed in the following.

C. Thermal equilibrium constraints

In the early universe, the WIMPs and SM particles are in thermal equilibrium. The reaction rates of WIMP pairs \leftrightarrow SM particles exceed the expansion rate of the universe,

$$\langle \sigma_{ann} v_r \rangle n_{eq} \gtrsim 1.66 \frac{\sqrt{g_*} T^2}{m_{Pl}}, \quad (24)$$

where n_{eq} is the corresponding equilibrium number density, with $n_f = 3\zeta(3)g_f T^3/4\pi^2$ for fermions in the relativistic limit. For SM particles \rightarrow WIMP pairs, the annihilation cross section of each fermion specie is

$$\sigma_{ann} v_r = \frac{\lambda_{SM}^2 k^2 \sqrt{1 - 4m_S^2/s}}{32\pi(s - 2m_f^2)} \frac{m_S^2(s - 4m_f^2)}{(s - m_\phi^2)^2}, \quad (25)$$

with $\lambda_{SM} \simeq \lambda_l \sin \theta m_q/v$ for charged leptons, quarks, respectively. The reaction rate can set a lower bound about the ϕ 's coupling to SM particles (see e.g. Refs. [46, 47] for more). If the mixing angle θ is tiny, with the contribution mainly from the $\tau\bar{\tau}$ annihilation, the reaction rate can give a lower bound on λ_τ . However, in this case, the WIMPs are insensitive in target nucleus scattering detections, and traces of ϕ are difficult to be observed at collider experiment. Here we focus on the interesting case of $t\bar{t}$ contribution dominating the SM particle reaction rate at $T \sim m_t$. By the calculation, we can obtain that the $t\bar{t}$ contribution is dominant when $\sin \theta$ is some times larger than $\sqrt{10}\lambda_\tau$ (this value corresponding to the nearly equal contributions of $t\bar{t}$ and $\tau\bar{\tau}$), e.g. $\sin \theta \gtrsim 10\lambda_\tau$. Moreover, an appreciable $\sin \theta$ value is available in interpreting the Galactic center gamma ray excess. Now, we have a range of θ ,

$$10\lambda_\tau \lesssim \sin \theta \lesssim 20\lambda_\tau. \quad (26)$$

For the case of the $t\bar{t}$ contribution dominating the SM reaction rate, according to Eq. (24), we obtain that the constraint can be written as

$$\sin^2 \theta k^2 m_S^2 (GeV) \gtrsim 2.2 \times 10^8 \frac{\pi^3 \sqrt{g_*} m_t}{\zeta(3) m_{Pl}} \approx 8.5 \times 10^{-7}. \quad (27)$$

This constraint is taken as the lower bound for the mixing angle θ and the parameter k . In fact, the constraint is valid for the WIMPs in a general mass range of $m_\phi < m_S \ll m_t$.

D. DM direct detection

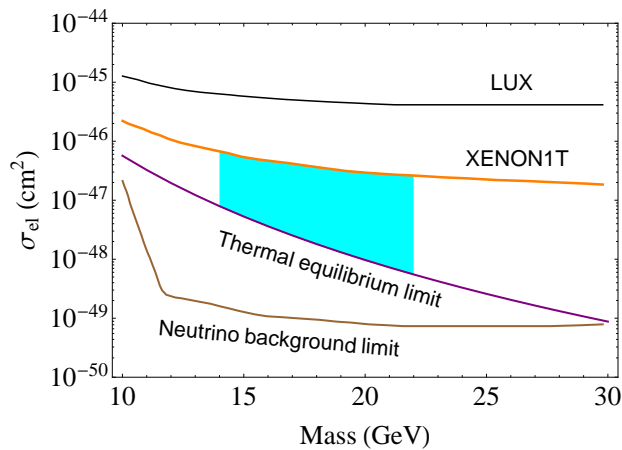


FIG. 3: The SI elastic cross section σ_{el} of WIMPs in a mass range 10 - 30 GeV. The solid curves from top to bottom are the upper limit set by LUX [3], the upper limit set by XENON1T [4], the lower limit set by the thermal equilibrium, the lower limit set by the neutrino background [49], respectively. The filled area is the allowed region of the elastic cross section in the potential mass range $m_S \sim 14 - 22$ GeV of concern.

Here we turn to the direct detection of WIMPs. The WIMP-target nucleus scattering is mainly mediated by ϕ . The effective coupling between ϕ and nucleon can be set by $\sin \theta g_{hNN}$, and g_{hNN} is the Higgs-nucleon coupling, with $g_{hNN} \simeq 1.71 \times 10^{-3}$ [48] adopted here. The cross section of the WIMP-nucleon SI elastic scattering is

$$\sigma_{el} \simeq \frac{\sin^2 \theta k^2 m_S^2 g_{hNN}^2 m_N^2}{4\pi(m_S + m_N)^2 m_\phi^4}, \quad (28)$$

where m_N is the nucleon mass.

For WIMPs in the mass range of concern, the recent DM searching results of LUX [3] and XENON1T [4] set stringent upper limits on the mixing angle θ and the parameter k . In addition, the thermal equilibrium condition requirement of Eq. (27) gives a lower bound on the parameters. Taking $m_\phi \sim m_S$, and considering the neutrino background [49] in detections, the tolerant hunting region of the cross section σ_{el} is depicted in Fig. 3, for WIMPs in an ordinary mass range 10 - 30 GeV. The filled region is for the potential mass range $m_S \sim 14 - 22$ GeV of concern,

which is indicated by the galactic center gamma ray excess, and the allowed region of the cross section is $\sigma_{\text{el}} \sim 10^{-48} - 10^{-46} \text{ cm}^2$. The parameter spaces are set by the thermal equilibrium limit and the recent XENON1T results. For $m_S \sim 14 - 22 \text{ GeV}$, the upper limit of XENON1T is fitted in the form

$$a \times (m_S)^b (\text{GeV}) \times \frac{g_{hNN}^2 m_N^2}{4\pi(m_S + m_N)^2 m_S^4}, \quad (29)$$

with the fitting values $a = (3.89 \pm 0.98) \times 10^{-10}$, $b = 3.71 \pm 0.09$. Thus, in the WIMP mass range of concern, the constraints of θ and k can be expressed as

$$8.5 \times 10^{-7} \lesssim \sin^2 \theta k^2 m_S^2 (\text{GeV}) \lesssim 2.61 \times 10^{-5} \left(\frac{m_S}{20}\right)^{3.71}. \quad (30)$$

This is the parameter space allowed, and it is detectable in DM direct detections in the future.

E. New sector search at collider

1. Higgs invisible decay

After the discovery of the SM-like Higgs boson at LHC [50, 51], the exploration of the Higgs portal new physics attracts much attention in recent years. In our scheme, the Higgs boson can decay into a WIMP pair, and the decay width is

$$\Gamma_{h \rightarrow S^* S} = \frac{\sin^2 \theta k^2 m_S^2}{16\pi m_h} \sqrt{1 - \frac{4m_\phi^2}{m_h^2}}. \quad (31)$$

Taking $m_h = 125 \text{ GeV}$ [52], the total width of SM Higgs is $4.07 \times 10^{-3} \text{ GeV}$ [39, 53]. With the constraints of the thermal equilibrium limit and the recent XENON1T results, i.e. Eq. (30), the branching ratio of Higgs boson decaying into a scalar WIMP pair is

$$3.3 \times 10^{-8} \lesssim \mathcal{B}_{h \rightarrow S^* S} \lesssim 1.0 \times 10^{-6} \left(\frac{m_S}{20}\right)^{3.71}. \quad (32)$$

This invisible branching ratio is very small and difficult to investigate at present and in the future collider experiment.

2. Production of ϕ

Now we turn to the ϕ production at collider. Due to the messy background at the hadron collider, the constraints from ATLAS [42] and CMS [43] are mild on the teens/tens GeV ϕ of concern, as discussed above. Here we focus on the search of ϕ at high energy e^+e^- collider, and this clean environment machine is good for high precise studies. The dominant production processes of ϕ are the ϕ -strahlung, the WW fusion, and the ZZ fusion, as depicted in Fig. 4.

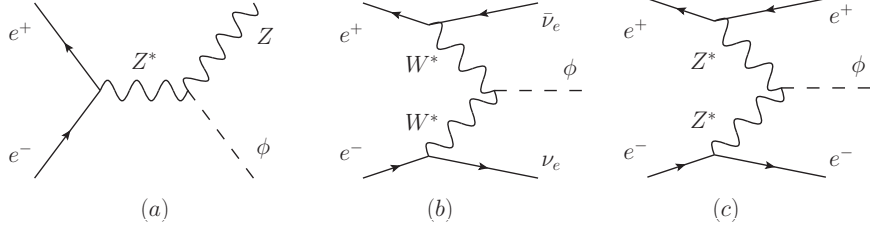


FIG. 4: The main production processes of ϕ at e^+e^- collider.

The ϕ strahlung process is similar to the case of Higgs boson production, and the corresponding cross section can be written as

$$\sigma_{e^+e^- \rightarrow Z\phi} = \frac{\sin^2 \theta G_F^2 m_Z^4}{96\pi s} (v_e^2 + a_e^2) \beta \frac{\beta^2 + 12m_Z^2/s}{(1 - m_Z^2/s)^2}, \quad (33)$$

where $G_F = 1.1663787(6) \times 10^{-5}$ GeV $^{-2}$ [39] is the Fermi coupling constant, and $v_e = -1 + 4\sin^2 \theta_W$, $a_e = -1$ are the vector, axial-vector current parameters, respectively. β is the phase space factor, with

$$\beta = \sqrt{\left(1 - \frac{m_\phi^2}{s} - \frac{m_Z^2}{s}\right)^2 - \frac{4m_\phi^2 m_Z^2}{s^2}}. \quad (34)$$

The cross section of the vector boson (WW , ZZ) fusion process can be written in the form [54–56]

$$\begin{aligned} \sigma &= \frac{\sin^2 \theta G_F^3 M_v^4}{64\sqrt{2}\pi^3} \int_{\kappa_\phi}^1 dx \int_x^1 \frac{dy}{[1 + (y-x)/\kappa_v]^2} [(\hat{v}^2 + \hat{a}^2)^2 f(x, y) + 4\hat{v}^2 \hat{a}^2 g(x, y)], \quad (35) \\ f(x, y) &= \left(\frac{2x}{y^3} - \frac{1+2x}{y^2} + \frac{2+x}{2y} - \frac{1}{2}\right) \left[\frac{z}{1+z} - \log(1+z)\right] + \frac{x}{y^3} \frac{z^2(1-y)}{1+z} \\ g(x, y) &= \left(-\frac{x}{y^2} + \frac{2+x}{2y} - \frac{1}{2}\right) \left[\frac{z}{1+z} - \log(1+z)\right] \end{aligned}$$

with $M_v = m_W, m_Z$ for the W, Z boson respectively, $\kappa_\phi = m_\phi^2/s$, $\kappa_v = M_v^2/s$, and $z = y(x - \kappa_\phi)/(x\kappa_v)$. \hat{v}, \hat{a} are the electron couplings to the vector bosons, with $\hat{v} = \hat{a} = \sqrt{2}$ for the W boson, and $\hat{v} = v_e$, $\hat{a} = a_e$ for the Z boson.

Let us give a further discussion about the range of θ before evaluating the production cross section of ϕ . From Eq. (16) and Eq. (30), we can derive a lower bound $\theta \gtrsim \theta_l$, with

$$\frac{6.1 \times 10^{-4}}{m_S^3} \lesssim \sin^2 \theta_l \lesssim \frac{1.9 \times 10^{-2}}{m_S^3} \left(\frac{m_S}{20}\right)^{3.71}. \quad (36)$$

In addition, θ should be much smaller than 1. As a rough estimate, an alteration of order 0.1% about the Higgs production and decay is tolerant by the present experiment. Here, an upper limit $\sin^2 \theta \lesssim 10^{-3}$ is taken. In SM particle scattering processes, the contribution from Higgs boson keeps dominant among the ϕ, h 's contributions.

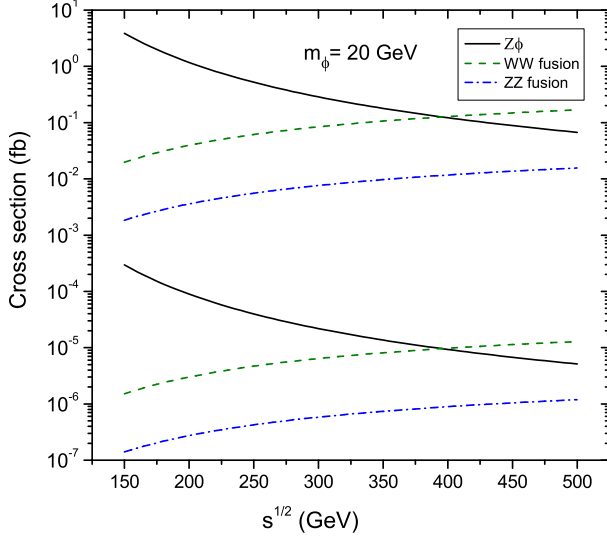


FIG. 5: The production cross section of ϕ at e^+e^- collider with $m_\phi = 20$ GeV and \sqrt{s} varying in a range of 150 - 500 GeV. The solid curves, the dashed curves and the dashed dotted curves are the production cross sections of the ϕ strahlung, WW fusion, and ZZ fusion, respectively. In each type curve, the upper one, the lower one are for the case of $\sin^2 \theta = 10^{-3}$, $\sin^2 \theta = 6.1 \times 10^{-4}/m_S^3$, respectively.

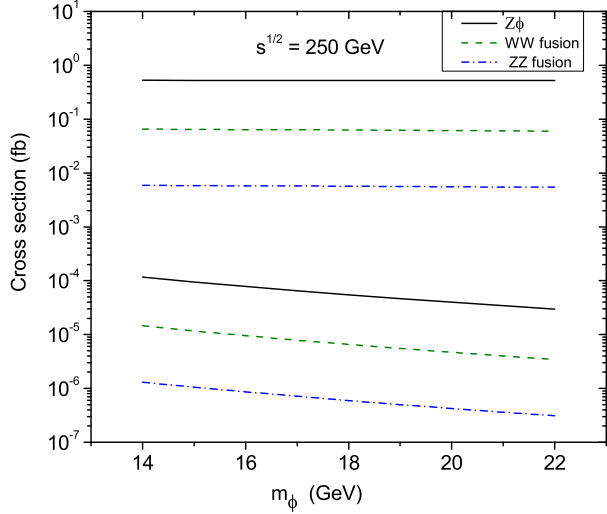


FIG. 6: The ϕ production cross section as a function of m_ϕ with m_ϕ varying in a range of 14 - 22 GeV at $\sqrt{s} = 250$ GeV. The solid curves, the dashed curves and the dashed dotted curves are the production cross sections of the ϕ strahlung, WW fusion, and ZZ fusion, respectively. In each type curve, the upper one, the lower one are for the case of $\sin^2 \theta = 10^{-3}$, $\sin^2 \theta = 6.1 \times 10^{-4}/m_S^3$, respectively.

With $m_\phi \sim m_S$ in this paper, we consider the production of ϕ in the range $m_\phi \sim 14$ - 22 GeV. Fixing $m_\phi = 20$ GeV, the dependence of the ϕ strahlung, WW fusion, and ZZ fusion cross sections with the center of mass energy \sqrt{s} is depicted in Fig. (5), for \sqrt{s} varying in a range 150 - 500 GeV. The upper limit, lower limit of the production cross sections are corresponding to $\sin^2 \theta = 10^{-3}$, $\sin^2 \theta = 6.1 \times 10^{-4}/m_S^3$, respectively. It can be seen that, for \sqrt{s} below 400

GeV, the main production process of ϕ is the ϕ strahlung mechanism. At a given center of mass energy $\sqrt{s} = 250$ GeV (the potential Higgs production energy), the production cross sections of ϕ for ϕ in the range 14 - 22 GeV is shown in Fig. (6), with the same upper limit, lower limit in the processes of ϕ strahlung, WW fusion, and ZZ fusion as that of Fig. (5). At the same $\sin^2 \theta$ value, the cross section changes slowly with m_ϕ . Thus, the upper limit results of ϕ production cross section given in Fig. (5) are roughly the cross section of ϕ with the mass of 14 - 22 GeV.

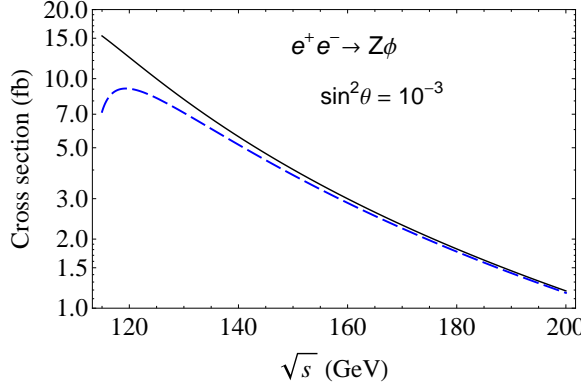


FIG. 7: The production cross section of ϕ as a function of \sqrt{s} in ϕ strahlung process at e^+e^- collider. The value $\sin^2 \theta = 10^{-3}$ is taken here, and \sqrt{s} varies in a range of 115 - 200 GeV. The solid curve, the dashed curve are for the case of $m_\phi = 14$ GeV, $m_\phi = 22$ GeV, respectively.

If the θ value is near the upper limit of the parameter space, the signature of ϕ may appear at the future high luminosity e^+e^- collider. Considering \sqrt{s} below 400 GeV, the main production mechanism of ϕ is via the ϕ strahlung. In the case $\sin^2 \theta = 10^{-3}$, there is about a hundred ϕ events produced at $\sqrt{s} = 250$ GeV with a integrated luminosity of 200 fb^{-1} . The dominant final state of ϕ is $\tau\bar{\tau}$, and the second branching fraction of $b\bar{b}$ final state is about 5% - 20%. The ϕ particle can be searched by the final states $(\phi \rightarrow \tau\bar{\tau})(Z \rightarrow q\bar{q})$, $(\phi \rightarrow b\bar{b})(Z \rightarrow l\bar{l}, q\bar{q})$. In fact, as shown in Fig. (7), it is better to test the non-standard model ϕ -like particle at a low center of mass energy collider with a high luminosity, e.g. $\sqrt{s} \sim 120$ - 150 GeV with the energy above the $Z\phi$ production threshold. For $\sin^2 \theta = 10^{-3}$, there are about 800 ($\sqrt{s} = 150$ GeV) - 2000 ($\sqrt{s} = 120$ GeV) ϕ production events with a integrated luminosity of 200 fb^{-1} . Thus, the new particle ϕ with θ near the upper limit of the parameter space can leave traces at the future high luminosity e^+e^- collider, or the upper limit of θ is reduced by the search result.

IV. ANALYSIS OF VECTORAL WIMPS

The vectoral WIMPs is similar to the case of scalar WIMPs. To satisfy the corresponding constraints, the value of ξ is approximately in the same range as the scalar WIMPs. The cross section of the vectoral WIMP-nucleon SI elastic scattering is

$$\sigma_{\text{el}} \simeq \frac{\sin^2 \theta k^2 m_V^2 g_{hNN}^2 m_N^2}{4\pi(m_V + m_N)^2 m_\phi^4}. \quad (37)$$

In the following, we just focus on the significant differences for vectoral WIMPs, and give a brief discussion about them.

For vectoral WIMPs, with $\xi \sim 0.994$, we have

$$|\lambda - 2k^2| \sim \sqrt{3} \times 2.0 \times 10^{-3} m_V (\text{GeV}) . \quad (38)$$

In the thermal equilibrium era of the early universe, the reaction rates of SM particles \rightarrow WIMP pairs exceed the expansion rate of the universe. The cross section of each SM fermion species annihilating into a vectoral WIMP pair is

$$\sigma_{ann} v_r = \frac{\lambda_{SM}^2 k^2 \sqrt{1 - 4m_V^2/s}}{32\pi(s - 2m_f^2)} \frac{m_V^2 (s - 4m_f^2)}{(s - m_\phi^2)^2} \left[2 + \frac{(s - 2m_V^2)^2}{4m_V^4} \right] . \quad (39)$$

At $T \sim m_t$, the reaction rates of SM particles are significantly enhanced by the longitudinal polarization of vectoral WIMPs, e.g. the enhancement over 10^5 for $t\bar{t}$. Consider the $t\bar{t}$ contribution dominating the SM particle reaction rate, and we have a range of θ ,

$$2\lambda_\tau \lesssim \sin \theta \lesssim 20\lambda_\tau . \quad (40)$$

The constraint of the thermal equilibrium can be approximately written as

$$\sin^2 \theta k^2 m_V^2 (\text{GeV}) \gtrsim 5.8 \times 10^2 \frac{\pi^3 \sqrt{g_*}}{\zeta(3) m_{\text{Pl}}} \left(\frac{m_t}{20} \right)^4 \approx 2.3 \times 10^{-12} \left(\frac{m_V}{20} \right)^4 . \quad (41)$$

For the vectoral WIMPs of concern, this thermal equilibrium constraint is below the neutrino background in DM direct detections, and the lower bound of the ϕ production cross section at e^+e^- collider is reduced by an order 10^{-5} factor compared with the case of scalar WIMPs.

V. CONCLUSION AND DISCUSSION

The scalar and vectoral WIMPs with a new scalar ϕ as the mediator have been explored in this article, for masses of WIMPs in a range about 14 - 22 GeV. The mass of ϕ is slightly below the WIMP mass, and the dominant annihilation products of WIMPs are on-shell $\phi\phi$ pairs, which mainly decay into $\tau\bar{\tau}$. The WIMP annihilation is phase space suppressed today. Considering the constraint of the DM relic density, the annihilation cross section $\langle \sigma_{ann} v_r \rangle_0 \sim 1 \times 10^{-26} \text{ cm}^3/\text{s}$ today can be obtained to meet the GeV gamma-ray excess.

The upper limit of the ϕ 's coupling to τ lepton is discussed with the constraints of WIMP annihilations, and the limit is tolerant by the muon $g - 2$ result. The scalar mediator-Higgs mixing angle θ is small enough to keep $\tau\bar{\tau}$ dominant in the scalar ϕ 's decay, and the upper limit of $\sin \theta$ from collider experiment is mild. The thermal equilibrium in the early universe sets a lower bound on the reaction rates of SM particles. Considering the $t\bar{t}$ contribution is dominant in SM particle reaction rates, we have derived a lower limit about the mixing angle θ and the coupling of the WIMP- ϕ trilinear term. For vectoral WIMPs, the reaction rate of $t\bar{t} \rightarrow$ WIMP pair is dramatically enhanced by the longitudinal polarization of vectoral WIMPs.

For the scalar WIMP-nucleon elastic scattering, the parameter spaces are set by the XENON1T result and the bound from thermal equilibrium. The allowed region of the elastic scattering cross section is derived, with $\sigma_{\text{el}} \sim 10^{-48} - 10^{-46} \text{ cm}^2$. The range of the scattering cross section can be examined at the future ultimate DM direct detection experiments, such as XENONnT [4] and DARWIN [57]. For vectoral WIMPs, the bound from thermal equilibrium is below the neutrino background in direct detections.

The Higgs boson can decay into a WIMP pair, while this invisible decay is tiny and difficult to be tested at collider. The main production cross sections of ϕ at e^+e^- collider are derived, i.e. the processes of ϕ strahlung, the WW fusion, and the ZZ fusion. For $\sqrt{s} < 400 \text{ GeV}$, the production of ϕ is mainly via the ϕ strahlung mechanism. The signature of ϕ with the θ value near the upper limit $\sin^2 \theta = 10^{-3}$ may appear at the future high luminosity e^+e^- collider, e.g. the Circular Electron Positron Collider (CEPC) [58], the International Linear Collider (ILC) [59], and FCC-ee(TLEP) [60]. It is better to test the non-standard model ϕ -like particle at a low center of mass energy collider with a high luminosity, e.g. $\sqrt{s} \sim 120 - 150 \text{ GeV}$ with the energy above the $Z\phi$ production threshold. We look forward to the future tests of the WIMPs of concern via DM indirections, DM direct detections and the hunt at collider.

Acknowledgments

Thank Xuewen Liu for useful discussions. This work was supported by the National Natural Science Foundation of China under Contract No. 11505144, and the Research Fund for the Doctoral Program of the Southwest University of Science and Technology under Contract No. 15zx7102.

-
- [1] G. Angloher *et al.* [CRESST Collaboration], *Eur. Phys. J. C* **76** (2016) no.1, 25 [[arXiv:1509.01515 \[astro-ph.CO\]](https://arxiv.org/abs/1509.01515)].
 - [2] R. Agnese *et al.* [SuperCDMS Collaboration], *Phys. Rev. Lett.* **116** (2016) no.7, 071301 [[arXiv:1509.02448 \[astro-ph.CO\]](https://arxiv.org/abs/1509.02448)].
 - [3] D. S. Akerib *et al.* [LUX Collaboration], *Phys. Rev. Lett.* **116** (2016) no.16, 161301 [[arXiv:1512.03506 \[astro-ph.CO\]](https://arxiv.org/abs/1512.03506)].
 - [4] E. Aprile *et al.* [XENON Collaboration], *JCAP* **1604** (2016) no.04, 027 [[arXiv:1512.07501 \[physics.ins-det\]](https://arxiv.org/abs/1512.07501)].
 - [5] K. N. Abazajian, N. Canac, S. Horiuchi and M. Kaplinghat, *Phys. Rev. D* **90** (2014) no.2, 023526 [[arXiv:1402.4090 \[astro-ph.HE\]](https://arxiv.org/abs/1402.4090)].
 - [6] T. Daylan, D. P. Finkbeiner, D. Hooper, T. Linden, S. K. N. Portillo, N. L. Rodd and T. R. Slatyer, *Phys. Dark Univ.* **12** (2016) 1 [[arXiv:1402.6703 \[astro-ph.HE\]](https://arxiv.org/abs/1402.6703)].
 - [7] F. Calore, I. Cholis and C. Weniger, *JCAP* **1503** (2015) 038 [[arXiv:1409.0042 \[astro-ph.CO\]](https://arxiv.org/abs/1409.0042)].
 - [8] D. Hooper and L. Goodenough, *Phys. Lett. B* **697** (2011) 412 [[arXiv:1010.2752 \[hep-ph\]](https://arxiv.org/abs/1010.2752)].
 - [9] T. Lacroix, C. Boehm and J. Silk, *Phys. Rev. D* **90** (2014) no.4, 043508 [[arXiv:1403.1987 \[astro-ph.HE\]](https://arxiv.org/abs/1403.1987)].
 - [10] Z. H. Yu, X. J. Bi, Q. S. Yan and P. F. Yin, *Phys. Rev. D* **91** (2015) no.3, 035008 [[arXiv:1410.3347 \[hep-ph\]](https://arxiv.org/abs/1410.3347)].

- [11] A. Ibarra and S. Wild, JCAP **1505** (2015) no.05, 047 [arXiv:1503.03382 [hep-ph]].
- [12] J. C. Park, S. C. Park and J. Kim, Phys. Lett. B **752** (2016) 59 [arXiv:1505.04620 [hep-ph]].
- [13] M. Ackermann *et al.* [Fermi-LAT Collaboration], Phys. Rev. Lett. **115** (2015) no.23, 231301 [arXiv:1503.02641 [astro-ph.HE]].
- [14] E. A. Baltz and L. Bergstrom, Phys. Rev. D **67** (2003) 043516 [hep-ph/0211325].
- [15] M. Pospelov and A. Ritz, Phys. Lett. B **671** (2009) 391 [arXiv:0810.1502 [hep-ph]].
- [16] C. R. Chen and F. Takahashi, JCAP **0902** (2009) 004 [arXiv:0810.4110 [hep-ph]].
- [17] I. Cholis, D. P. Finkbeiner, L. Goodenough and N. Weiner, JCAP **0912** (2009) 007 [arXiv:0810.5344 [astro-ph]].
- [18] P. J. Fox and E. Poppitz, Phys. Rev. D **79** (2009) 083528 [arXiv:0811.0399 [hep-ph]].
- [19] Q. H. Cao, E. Ma and G. Shaughnessy, Phys. Lett. B **673** (2009) 152 [arXiv:0901.1334 [hep-ph]].
- [20] X. J. Bi, X. G. He and Q. Yuan, Phys. Lett. B **678** (2009) 168 [arXiv:0903.0122 [hep-ph]].
- [21] A. Ibarra, A. Ringwald, D. Tran and C. Weniger, JCAP **0908** (2009) 017 [arXiv:0903.3625 [hep-ph]].
- [22] J. Kopp, V. Niro, T. Schwetz and J. Zupan, Phys. Rev. D **80** (2009) 083502 [arXiv:0907.3159 [hep-ph]].
- [23] T. Cohen and K. M. Zurek, Phys. Rev. Lett. **104** (2010) 101301 [arXiv:0909.2035 [hep-ph]].
- [24] A. Rajaraman, J. Smolinsky and P. Tanedo, arXiv:1503.05919 [hep-ph].
- [25] J. M. Cline, G. Dupuis, Z. Liu and W. Xue, Phys. Rev. D **91** (2015) no.11, 115010 [arXiv:1503.08213 [hep-ph]].
- [26] O. Adriani *et al.* [PAMELA Collaboration], Phys. Rev. Lett. **105** (2010) 121101 [arXiv:1007.0821 [astro-ph.HE]].
- [27] L. Bergstrom, T. Bringmann, I. Cholis, D. Hooper and C. Weniger, Phys. Rev. Lett. **111** (2013) 171101 [arXiv:1306.3983 [astro-ph.HE]].
- [28] D. Hooper and W. Xue, Phys. Rev. Lett. **110** (2013) no.4, 041302 [arXiv:1210.1220 [astro-ph.HE]].
- [29] A. Ibarra, A. S. Lamperstorfer and J. Silk, Phys. Rev. D **89** (2014) no.6, 063539 [arXiv:1309.2570 [hep-ph]].
- [30] M. Pospelov, A. Ritz and M. B. Voloshin, Phys. Lett. B **662** (2008) 53 [arXiv:0711.4866 [hep-ph]].
- [31] B. Batell, D. McKeen and M. Pospelov, JHEP **1210** (2012) 104 [arXiv:1207.6252 [hep-ph]].
- [32] J. Liu, N. Weiner and W. Xue, JHEP **1508** (2015) 050 [arXiv:1412.1485 [hep-ph]].
- [33] J. Abdallah *et al.*, Phys. Dark Univ. **9-10** (2015) 8 [arXiv:1506.03116 [hep-ph]].
- [34] E. W. Kolb and M. S. Turner, The Early Universe, Front. Phys. **69** (1990) 1.
- [35] K. Griest and D. Seckel, Phys. Rev. D **43** (1991) 3191.
- [36] P. Gondolo and G. Gelmini, Nucl. Phys. B **360** (1991) 145.
- [37] M. Cannoni, Phys. Rev. D **89** (2014) no.10, 103533 [arXiv:1311.4494 [astro-ph.CO], arXiv:1311.4508 [astro-ph.CO]].
- [38] P. A. R. Ade *et al.* [Planck Collaboration], arXiv:1502.01589 [astro-ph.CO].
- [39] K. A. Olive *et al.* [Particle Data Group Collaboration], Chin. Phys. C **38** (2014) 090001.
- [40] A. Hektor, K. Kannike and L. Marzola, JCAP **1510** (2015) no.10, 025 [arXiv:1507.05096 [hep-ph]].
- [41] R. Barate *et al.* [LEP Working Group for Higgs boson searches and ALEPH and DELPHI and L3 and OPAL Collaborations], Phys. Lett. B **565** (2003) 61 [hep-ex/0306033].
- [42] [ATLAS Collaboration], ATLAS-CONF-2011-020.
- [43] S. Chatrchyan *et al.* [CMS Collaboration], Phys. Rev. Lett. **109** (2012) 121801 [arXiv:1206.6326 [hep-ex]].
- [44] J. D. Clarke, R. Foot and R. R. Volkas, JHEP **1402** (2014) 123 [arXiv:1310.8042 [hep-ph]].

- [45] U. Haisch and J. F. Kamenik, Phys. Rev. D **93** (2016) no.5, 055047 [arXiv:1601.05110 [hep-ph]].
- [46] X. Chu, T. Hambye and M. H. G. Tytgat, JCAP **1205** (2012) 034 [arXiv:1112.0493 [hep-ph]].
- [47] M. J. Dolan, F. Kahlhoefer, C. McCabe and K. Schmidt-Hoberg, JHEP **1503** (2015) 171 Erratum: [JHEP **1507** (2015) 103] [arXiv:1412.5174 [hep-ph]].
- [48] X. G. He, T. Li, X. Q. Li, J. Tandean and H. C. Tsai, Phys. Rev. D **79** (2009) 023521 [arXiv:0811.0658 [hep-ph]].
- [49] J. Billard, L. Strigari and E. Figueroa-Feliciano, Phys. Rev. D **89** (2014) no.2, 023524 [arXiv:1307.5458 [hep-ph]].
- [50] G. Aad *et al.* [ATLAS Collaboration], Phys. Lett. B **716** (2012) 1 [arXiv:1207.7214 [hep-ex]].
- [51] S. Chatrchyan *et al.* [CMS Collaboration], Phys. Lett. B **716** (2012) 30 [arXiv:1207.7235 [hep-ex]].
- [52] G. Aad *et al.* [ATLAS and CMS Collaborations], Phys. Rev. Lett. **114** (2015) 191803 [arXiv:1503.07589 [hep-ex]].
- [53] A. Denner, S. Heinemeyer, I. Puljak, D. Rebuzzi and M. Spira, Eur. Phys. J. C **71** (2011) 1753 [arXiv:1107.5909 [hep-ph]].
- [54] Proceedings of the Workshop e^+e^- Collisions at 500 GeV: The Physics Potential, Munich-Annecy-Hamburg, ed. P. M. Zerwas, Reports DESY 92-123A,B;93-123C.
- [55] W. Kilian, M. Kramer and P. M. Zerwas, Phys. Lett. B **373** (1996) 135 [hep-ph/9512355].
- [56] A. Djouadi *et al.*, In *Annecy/Gran Sasso/Hamburg 1995, $e^+ e^-$ collisions at TeV energies: The physics potential. Pt. D* 95-97 [hep-ph/9605437].
- [57] J. Aalbers *et al.* [DARWIN Collaboration], arXiv:1606.07001 [astro-ph.IM].
- [58] The CEPC Study Group, CEPC-SppC Preliminary Conceptual Design Report: Physics and Detector. Website: <http://cepc.ihep.ac.cn>
- [59] H. Baer *et al.*, The International Linear Collider Technical Design Report - Volume 2: Physics, arXiv:1306.6352 [hep-ph].
- [60] M. Bicer *et al.* [TLEP Design Study Working Group Collaboration], JHEP **1401** (2014) 164 [arXiv:1308.6176 [hep-ex]].